Beneficial Microbes, 2018; 9 (5): 799-814

Wageningen Academic Publishers

Gut bacterial composition in a mouse model of Parkinson's disease

P. Perez-Pardo[1], H.B. Dodiya[2], P.A. Engen[2], A. Naqib[3], C.B. Forsyth[2], S.J. Green[3], J. Garssen[1,4], A. Keshavarzian[2] and A.D. Kraneveld[1,5*]

[1]Division of Pharmacology, Utrecht Institute for Pharmaceutical Sciences, Faculty of Science, Utrecht University, Universiteitsweg 99, 3584 CG Utrecht, the Netherlands; [2]Department of Internal Medicine, Division of Digestive Disease and Nutrition, Rush University Medical Center, 1725 West Harrison Street, Chicago, IL 60612, USA; [3]DNA Services Facility, University of Illinois, 835 S Wolcott, Chicago, IL 60612, USA; [4]Nutricia Research, Uppsalalaan 12, 3584 CT Utrecht, the Netherlands; [5]Institute for Risk Assessment Sciences, Faculty of Veterinary Medicine, Utrecht University, Yalelaan 104, 3584 CM Utrecht, the Netherlands; a.d.kraneveld@uu.nl

Received: 21 December 2017 / Accepted: 23 March 2018

RESEARCH ARTICLE

Abstract

The mechanism of neurodegeneration in Parkinson's disease (PD) remains unknown but it has been hypothesised that the intestinal tract could be an initiating and contributing factor to the neurodegenerative processes. In PD patients as well as in animal models for PD, alpha-synuclein-positive enteric neurons in the colon and evidence of colonic inflammation have been demonstrated. Moreover, several studies reported pro-inflammatory bacterial dysbiosis in PD patients. Here, we report for the first time significant changes in the composition of caecum mucosal associated and luminal microbiota and the associated metabolic pathways in a rotenone-induced mouse model for PD. The mouse model for PD, induced by the pesticide rotenone, is associated with an imbalance in the gut microbiota, characterised by a significant decrease in the relative abundance of the beneficial commensal bacteria genus *Bifidobacterium*. Overall, intestinal bacterial dysbiosis might play an important role in both the disruption of intestinal epithelial integrity and intestinal inflammation, which could lead or contribute to the observed alpha-synuclein aggregation and PD pathology in the intestine and central nervous system in the oral rotenone mouse model of PD.

Keywords: microbiota, dysbiosis, rotenone, caecum, neurodegeneration

1. Introduction

Parkinson's disease (PD) is the second most common adult neurodegenerative disease after Alzheimer's disease, characterised by motor impairments due to defects in motor control (De Rijk *et al.*, 2000; Nussbaum and Ellis, 2003). The main hallmarks of this disease in the brain are the progressive degeneration of dopaminergic nigrostriatal neurons and the presence of misfolded, aggregated and neurotoxic forms of the protein alpha-synuclein in the remaining neurons (Crossman, 1989). Several studies have demonstrated that neuroinflammation and oxidative stress are the key factors responsible for alpha-synuclein misfolding and aggregation (Deleidi and Gasser, 2013; Dias *et al.*, 2013; Glass *et al.*, 2010; Luna and Luk, 2015; Ransohoff, 2016). The source of this inflammatory state is not well established. However, multiple experimental and clinical observations strongly suggest that the intestine could be the primary source of neuro-inflammation. For example, besides the brain pathology, PD patients also develop non-motor symptoms, including gastrointestinal (GI) dysfunctions (Fasano *et al.*, 2015; Pfeiffer, 2011). These GI symptoms include constipation that may precede the motor symptoms by several years, and chronic constipation in otherwise healthy people is associated with an increased risk of developing PD (Abbott *et al.*, 2001; Adams-Carr *et al.*, 2016). Moreover, GI dysfunctions are major determinants for the quality of life (Martinez-Martin, 2011; Müller *et al.*, 2013) and remain undertreated (Chaudhuri and Schapira, 2009). Furthermore, in PD patients, as well as in animal models for PD, alpha-synuclein-positive enteric neurons in intestinal mucosal samples have been

found (Hilton *et al.*, 2014; Kelly *et al.*, 2014; Perez-Pardo *et al.*, 2017; Shannon *et al.*, 2012; Stokholm *et al.*, 2016), although the data remains controversial for their specificity to PD patients only (Visanji *et al.*, 2015). In PD patients, alpha-synuclein-positive structures in the colonic mucosa were detected from 2 to 5 years before the onset of motor symptoms (Shannon *et al.*, 2012) and in another cohort of PD patients, alpha-synuclein was significantly associated with abnormal intestinal permeability and endotoxemia (Forsyth *et al.*, 2011). In the oral rotenone-induced mouse model for PD, enteric alpha-synuclein aggregates and intestinal inflammation were associated with reduced intestinal transit (Perez-Pardo *et al.*, 2017).

Indeed, Braak was the first investigator to propose the gastrointestinal tract (GIT) as the primary source to trigger neuro-inflammation and neurodegeneration leading to PD pathology and cardinal symptoms of PD (Braak and Del Tredici, 2008; Hawkes *et al.*, 2009). He proposed that environmental putative pathogens can access through the GIT disrupting enteric nervous system (ENS) leading to alpha-synuclein pathology which could reach to the brain in a prion-like fashion (Braak and Del Tredici, 2008; Hawkes *et al.*, 2009). Besides environmental putative pathogens, other possible mechanism/s for the intestine to trigger and promote neuro-inflammation is abnormal microbiota composition (so called pro-inflammatory dysbiosis) and/or disruption of intestinal barrier integrity (so called leaky gut) leading to exposure of pro-inflammatory bacteria/bacterial products to ENS (Hawkes *et al.*, 2010) and even central nervous system (CNS) (Guan *et al.*, 2013). Indeed, the GIT, especially colon, harbours one of the most complex and diverse bacterial community. Disruption in the intestinal microbiota community (dysbiosis), by genetic and environmental factors, have been associated with a wide range of neurodegenenerative disorders, including PD (Bedarf *et al.*, 2017; Hasegawa *et al.*, 2015; Hill-Burns *et al.*, 2017; Hopfner *et al.*, 2017; Keshavarzian *et al.*, 2015; Li *et al.*, 2017; Petrov *et al.*, 2017; Scheperjans *et al.*, 2015; Unger *et al.*, 2016).

Although dysbiosis has now been reported in PD, it is not yet clear whether changes in the microbiota community structure is a trigger for PD pathology. Animal models can provide an opportunity to look for this causal link. Indeed, our group showed that transplantation of stool from PD patients to germ-free alpha-synuclein transgenic mice triggered PD like motor deficits and CNS pathologies, suggesting that dysbiotic intestinal microbiota can trigger PD pathology in a genetically susceptible host (Sampson *et al.*, 2016).

Orally gavaged rotenone mice recapitulate many aspects of PD including PD like motor deficit, intestinal dysfunction (such as slow transit and constipation), alpha-synuclein pathology in the intestine and CNS, central and intestinal inflammation, and nigral neurodegeneration (Perez-Pardo *et al.*, 2017). Thus, we posit that the low-dose oral rotenone is an appropriate model to interrogate the role of microbiota gut-brain axis in PD. We hypothesise that rotenone treated mice have dysbiosis and the observed intestinal phenotype, such as disrupted intestinal barrier, inflammation, alpha-synuclein accumulation in ENS and intestinal transit deficits in these mice are associated with an altered intestinal microbiota composition. Accordingly, we interrogated caecum mucosal-associated and luminal microbiota compositions in rotenone treated mice and correlated microbiota to their intestinal outcomes. We found that low-dose oral rotenone treatment leads to dysbiotic mucosal and luminal microbiota structures and these changes are significantly correlated with intestinal symptoms in our model.

2. Materials and methods

Animal housing

Seven week old C57BL/6J male mice (Jackson Laboratories, Bar Harbor, ME, USA) were housed under a 12 h light/dark cycle. Food and water were provided *ad libitum*. Animal procedures were approved by the Ethical Committee of Animal Research of Utrecht University, Utrecht, the Netherlands.

Induction of mitochondrial dysfunction by rotenone in mice

Mice received freshly prepared rotenone (Sigma-Aldrich, Zwijndrecht, the Netherlands) solution (10 mg/kg body weight; suspended freshly in 4% carboxymethylcellulose (Sigma-Aldrich) and 1.25% chloroform (vehicle) once a day for 28 days by oral gavage as described before (Perez-Pardo *et al.*, 2017). Control animals received vehicle. On day 28, mice were sacrificed by decapitation and the brain and the intestinal tissue were collected for further analysis.

Immunohistochemistry and image analysis

Antibodies for ZO-1 (ab59720, Abcam, Cambridge, UK), glial fibrillary acidic protein (Z0334, Dako, Glostrup, Denmark), CD3 (ab49943, Abcam) and alpha-synuclein (04-1053, Millipore, Burlington, MA, USA) were used to evaluate the gut pathology in the different experimental groups. Data collection for tight junction barrier integrity analyses (ZO-1 integrity) and stereology analyses were performed as described before (Perez-Pardo *et al.*, 2017). The brains were stained with tyrosine hydroxylase (TH) (sc-14007, Santa Cruz Biotechnology, Dallas, TX, USA) and iba-1 (019-197410, Wako Pure Chemical, Osaka, Japan) antibodies to assess the amount of dopaminergic neurons and microglia morphology in the substantia nigra (SN). TH-immunopositive neurons were assessed using stereology counting as previously described (Perez-Pardo *et al.*, 2017).

For microglia analysis z-stacks were imaged at 1µm step and analysed with Image-J software (https://imagej.net). The experimenter designates individual cells and the software quantified the number of branches, the number of branches endpoints, the branch length, the cell body size and the total cell size. 20 cells per region per animal were analysed.

Microbiota profiling and bioinformatic analyses

We chose the caecum as our site of investigation, based on our previously characterised data on the small intestine in this PD mouse model (Perez-Pardo *et al.*, 2017). Also, the caecum is a major site of bacterial fermentation (Brown *et al.*, 2017). We chose to interrogate both mucosal associated and luminal microbiota communities because each of these two compartments have unique microbiota communities (Carroll *et al.*, 2011; Durbán *et al.*, 2011; Engen *et al.*, 2017; Keshavarzian *et al.*, 2015) with different impacts on the host (Kostic *et al.*, 2013). For example, mucosal associated microbiota could have more impact on mucosal barrier integrity (Huang *et al.*, 2013) and immunity (McDermott and Huffnagle, 2014); while fermentation products of luminal microbiota community, like short chain fatty acids (SCFA), can have a different impact on the host (Basson *et al.*, 2016; Canani *et al.*, 2011).

Total DNA was extracted from both mice caecum mucosa and caecum luminal content samples (FastDNA bead-beating Spin Kit for Soil, MP Biomedicals, Solon, OH, USA), amplified the V4 variable region of the microbial 16S rRNA gene (Earth Microbiome Project primer set, adapted for the Illumina platform, San Diego, CA, USA) (Caporaso *et al.*, 2012), and sequenced on an Illumina MiSeq (2×151 bp reads) at Argonne National Laboratory. Negative controls were used with each set of amplifications, which indicated no contamination. The raw sequence data (FASTQ files) were deposited in the National Center for Biotechnology Information (NCBI) Sequence Read Archive (SRA), under the BioProject identifier PRJNA387564.

Forward and reverse reads were merged, quality trimmed and sequences shorter than 250 bases were discarded (CLC Genomics Workbench, v7.0, CLC Bio, Qiagen, Boston, MA, USA). Sequences were screened for chimeras (usearch61 algorithm) (Edgar, 2010), and putative chimeric sequences were removed from the dataset (QIIME v1.8.) (Caporaso *et al.*, 2010). Each sample sequence set was rarefied to 25,000 sequences (Gihring *et al.*, 2012) and data were pooled, renamed, and clustered into operational taxonomic units (OTU) at 97% similarity (usearch61algorithm). Representative sequences from each OTU were extracted and classified using the uclust consensus taxonomy assigner (Greengenes 13_8 reference database). A biological observation matrix (McDonald *et al.*, 2012) was generated at each taxonomic level ('make OTU table' algorithm) and analysed and visualised using Primer7 (Clarke, 1993).

Classification of putative 'pro-inflammatory' and putative 'anti-inflammatory' bacteria taxa were based on preceding reports (Canani *et al.*, 2011; Hakansson and Molin, 2011; Louis and Flint, 2009; MacFarlane and MacFarlane, 2003; Wexler, 2007).

Statistical analyses

Alpha diversity indices (within-sample) and beta diversity (between-sample) were used to examine changes in microbial community structure between mice group samples. Alpha diversity indices (i.e. Shannon, Simpson, richness, and evenness) were generated using the package 'vegan' implemented in the *R* programming language. To examine differences in community composition between samples, pairwise Bray-Curtis dissimilarity (non-phylogenetic) metric was generated using the Primer7 software package and used to perform analysis of similarity (ANOSIM) calculations; ANOSIM and non-metric multidimensional scaling (nMDS) plots were performed at the taxonomic level of family, using non-transformed data.

The differences in the relative abundance of individual taxa between defined groups were assessed for significance using Kruskal-Wallis test controlling for false-discovery rate (FDR) corrected p-value, implemented within the software package QIIME (Caporaso *et al.*, 2010). Taxa with an average abundance of <1% across the sample set were removed from the analysis. Microbial relative abundances and *Firmicutes*/*Bacteroidetes* (F/B) ratios between conditions were studied. The relative abundance of individual taxa reported in our mouse model was accepted at a significance of (FDR-P<0.05).

Mice caecum mucosa and caecum content sample's community functional predictions were performed using PICRUSt to infer microbiota function (Phylogenetic Investigation of Communities by Reconstruction of Unobserved States) (Langille *et al.*, 2013). Differences in Kyoto Encyclopedia of Genes and Genomes (KEGG) ortholog (KO) abundances between groups were identified (Kruskal-Wallis test) (Kanehisa and Goto, 2000). KEGG pathways were analysed using the KEGG Mapper pathway search function (Kanehisa *et al.*, 2012). PICRUSt analysis significance was accepted at (FDR-P<0.05).

In SPSS (V.22) (SPSS, Inc., Chicago, IL, USA), two factor analysis of variance (2-way ANOVA), with a Bonferroni post-hoc test, was used to analyse differences for parametric data satisfying test assumptions for alpha diversity indices. Pearson correlations were applied to associate the different symptoms developed with rotenone exposure in mice. These collective test results were considered statistically significant at (P<0.05). All graphs were created using GraphPad Prism (v5.00; La Jolla, CA, USA) software.

3. Results

Mucosal associated and luminal bacteria in a rotenone-induced mouse model for PD

We assessed microbiota community structure in rotenone treated mice using both alpha and beta diversity analyses. We found that both mucosal associated and luminal microbiota community structure is impacted in rotenone treated mice. The caecal mucosa's richness was significantly increased in rotenone-treated mice compared to vehicle-treated mice (2-way ANOVA: (treatment) $F_{(1,38)}$=14.90, P<0.0001; (Bonferroni Post-Hoc=P<0.01) (Figure 1A); while alpha diversity (Shannon index, Simpson index and evenness) were not affected by rotenone treatment (Figure 1B, 1C and 1D). Furthermore, the luminal (caecal content) microbiota showed no significant differences in alpha diversity indices between rotenone-treated and vehicle-treated mice (data not shown).

Upon examining the beta diversity, at the taxonomic level of family, the overall microbial community structure in the caecal mucosa of rotenone-treated mice was significantly different from vehicle-treated mice (ANOSIM: Global R=0.635; P=0.001) (Figure 2A). Similar effects were observed in the luminal (caecal content) microbiota community composition of rotenone-treated mice (ANOSIM: Global R=0.734; P=0.001) (Figure 2B).

At different taxonomic levels (phylum, family, and genus), individual taxa showed significant differences in both sample sites of the vehicle and rotenone treated mice groups (Table 1 and Figure 3). Within the caecal mucosa, rotenone-treated mice showed a significant increase in the relative abundances of the phylum *Bacteroidetes* (FDR-P<0.01) and *Firmicutes* (FDR-P<0.001), with a decrease in the relative abundance of *Actinobacteria* (FDR-P<0.001), compared to vehicle-treated mice (Table 1). However, when the caecal content was examined, the rotenone-treated mice showed a significantly higher relative abundance of the phylum *Firmicutes* (FDR-P<0.001), and a lower relative abundance of *Actinobacteria* (FDR-P<0.001) (Table 1). Additionally, the caecal mucosa *Firmicutes*-to-*Bacteroidetes* (F/B) ratio indicated a significant rotenone effect (2-way ANOVA: (treatment) $F_{(1,38}$)=7.502, P<0.010) and lower F/B ratio (Bonferroni post-hoc: P<0.05) in the rotenone-treated mice compared to vehicle-treated mice (Figure 4). For the caecal content, the F/B ratio showed no significant difference between groups (Figure 4).

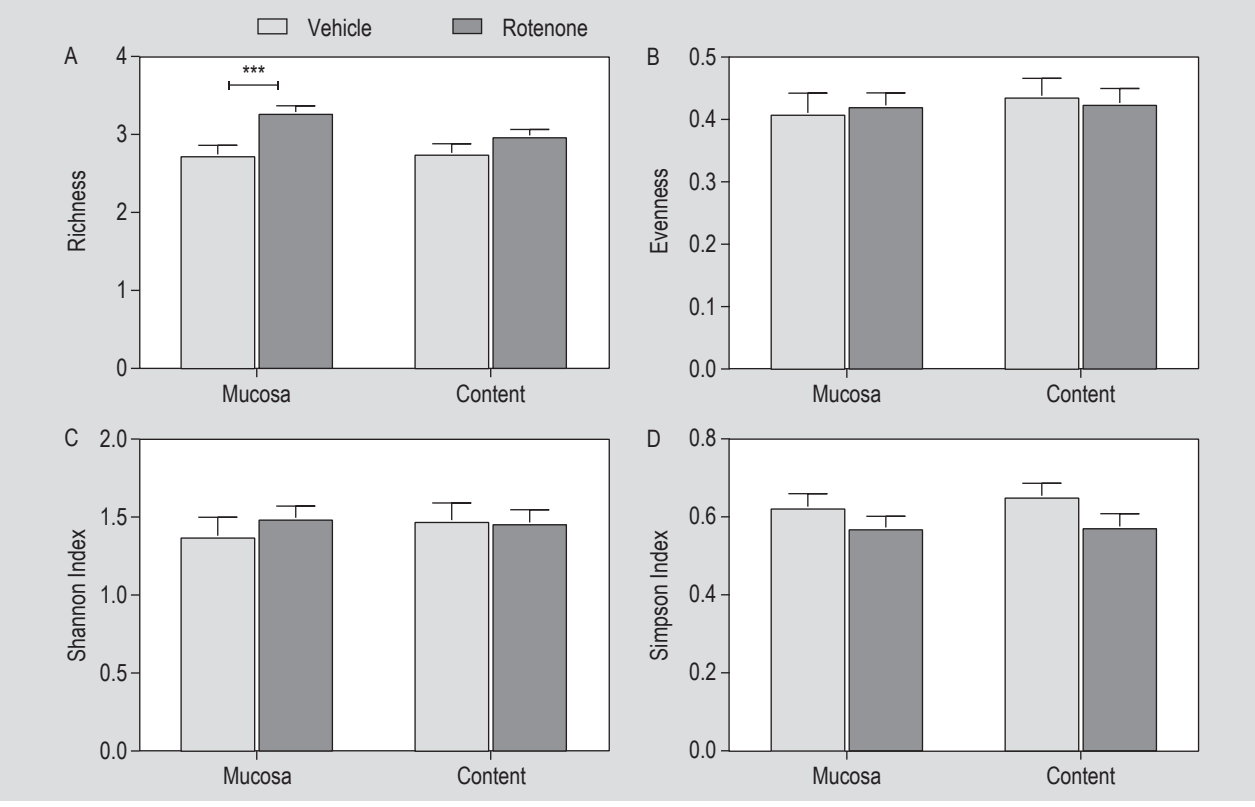

Figure 1. Alpha diversity (within samples) comparisons between vehicle (white bars) and rotenone (black bars) treatments in mice in caecal mucosa and content, at the taxonomic level of family. (A) richness; (B) evenness; (C) Shannon index; (D) Simpson index. Data expressed as mean + standard error of the mean and analysed with 2-way ANOVA, Bonferroni post-hoc test for n=9-10 per group; ** *P*<0.01 (site); * *P*<0.001 (treatment).**

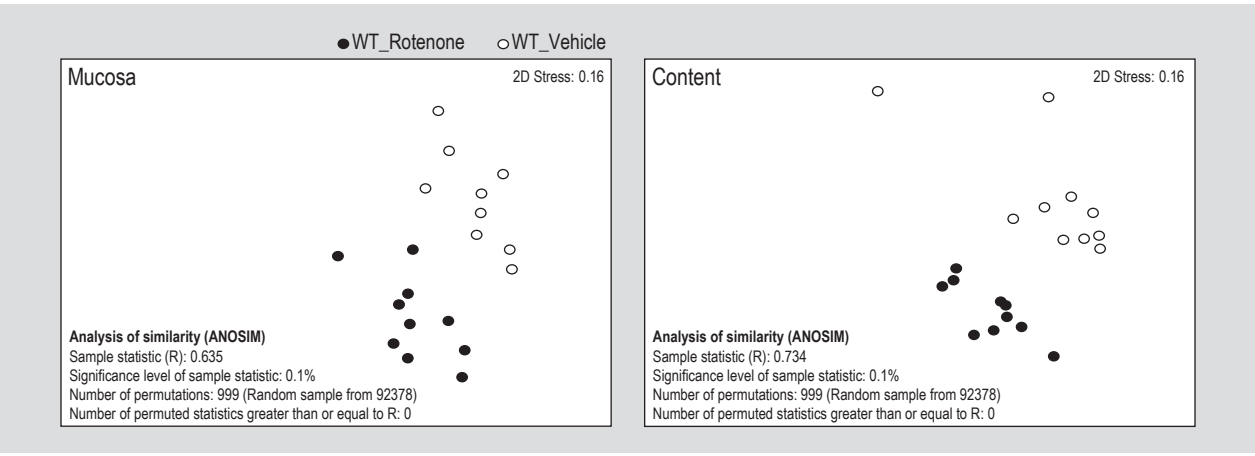

Figure 2. Ordination plots (nMDS plots) of microbial community structure at the taxonomic level of family, using analysis of similarity ANOSIM, comparing vehicle (white dots) and rotenone (black dots) treated mice caecal mucosa (A) and content (B), n=9-10 mice per group.

Table 1. Rotenone-associated relative abundance individual taxa changes within mice caecal mucosa and content.[1,2]

		Caecal mucosa			Caecal content		
		Vehicle	Rotenone	Veh vs Rot FDR-*P*	Vehicle	Rotenone	Veh vs Rot FDR-*P*
Phylum	*Actinobacteria*	7,109.20	2,226.00	0.00	6,987.90	3,505.20	0.00
	Bacteroidetes	540.50	1,606.70	0.01	810.90	1,221.40	0.29
	Firmicutes	15,572.20	19,782.60	0.00	15,334.90	19,102.00	0.00
	Proteobacteria	1,181.80	629.00	0.76	1,204.60	452.20	0.32
	Unassigned; other	490.60	533.40	0.76	614.60	637.40	0.76
Family	*Actinobacteria; Bifidobacteriaceae*	6,731.80	1,835.20	0.00	6,453.00	2,069.60	0.01
	Actinobacteria; Coriobacteriaceae	392.00	383.60	0.68	545.70	1,456.20	0.82
	Bacteroidetes; Rikenellaceae	63.10	476.10	0.00	87.40	423.60	0.01
	Bacteroidetes; S24-7	356.90	860.70	0.01	533.20	578.70	0.48
	Firmicutes; Clostridiales (o)	892.60	1,663.40	0.01	1,182.40	1,453.90	0.18
	Firmicutes; Erysipelotrichaceae	13,190.20	15,885.00	0.01	12,496.90	15,862.30	0.06
	Firmicutes; Lachnospiraceae	423.20	589.10	0.06	617.10	536.00	0.48
	Firmicutes; Lactobacillaceae	790.80	737.20	0.88	654.30	583.20	0.82
	Firmicutes; Ruminococcaceae	222.70	508.30	0.01	296.50	435.20	0.18
	Proteobacteria; Desulfovibrionaceae	922.40	612.40	0.88	1,089.90	444.70	0.56
	Unassigned; other	489.40	526.40	0.88	609.40	633.00	0.82
Genus	*Actinobacteria; Bifidobacteriaceae; Bifidobacterium*	6,734.70	1,830.30	0.00	6,448.60	2,074.60	0.01
	Actinobacteria; Coriobacteriaceae; g	280.90	288.60	0.97	395.60	1,321.50	0.62
	Bacteroidetes; Rikenellaceae; g	59.70	469.20	0.00	85.20	418.30	0.01
	Bacteroidetes; S24-7; g	354.10	854.40	0.02	536.20	588.10	0.51
	Firmicutes; Clostridiales (o); f; g	891.70	1,661.90	0.02	1,186.80	1,468.70	0.24
	Firmicutes; Erysipelotrichaceae; Allobaculum	13,166.10	15,878.10	0.02	12,476.80	15,843.60	0.06
	Firmicutes; Lachnospiraceae; g	290.40	312.00	0.13	397.00	286.30	0.51
	Firmicutes; Lactobacillaceae; Lactobacillus	784.70	734.10	0.97	659.50	583.10	0.78
	Proteobacteria; Desulfovibrionaceae; Desulfovibrio	913.10	567.70	0.97	1,070.50	421.30	0.62
	Unassigned; other; other	489.30	534.50	0.97	613.60	633.10	0.82

[1] Group-significant testing was performed using Kruskal-Wallis test plus false discovery rate correction (FDR-*P*), n=9-10 mice per group. Significant *P*<0.05; trend *P*<0.1.

[2] (o) = order; f = unspecified family, g = unspecified genus.

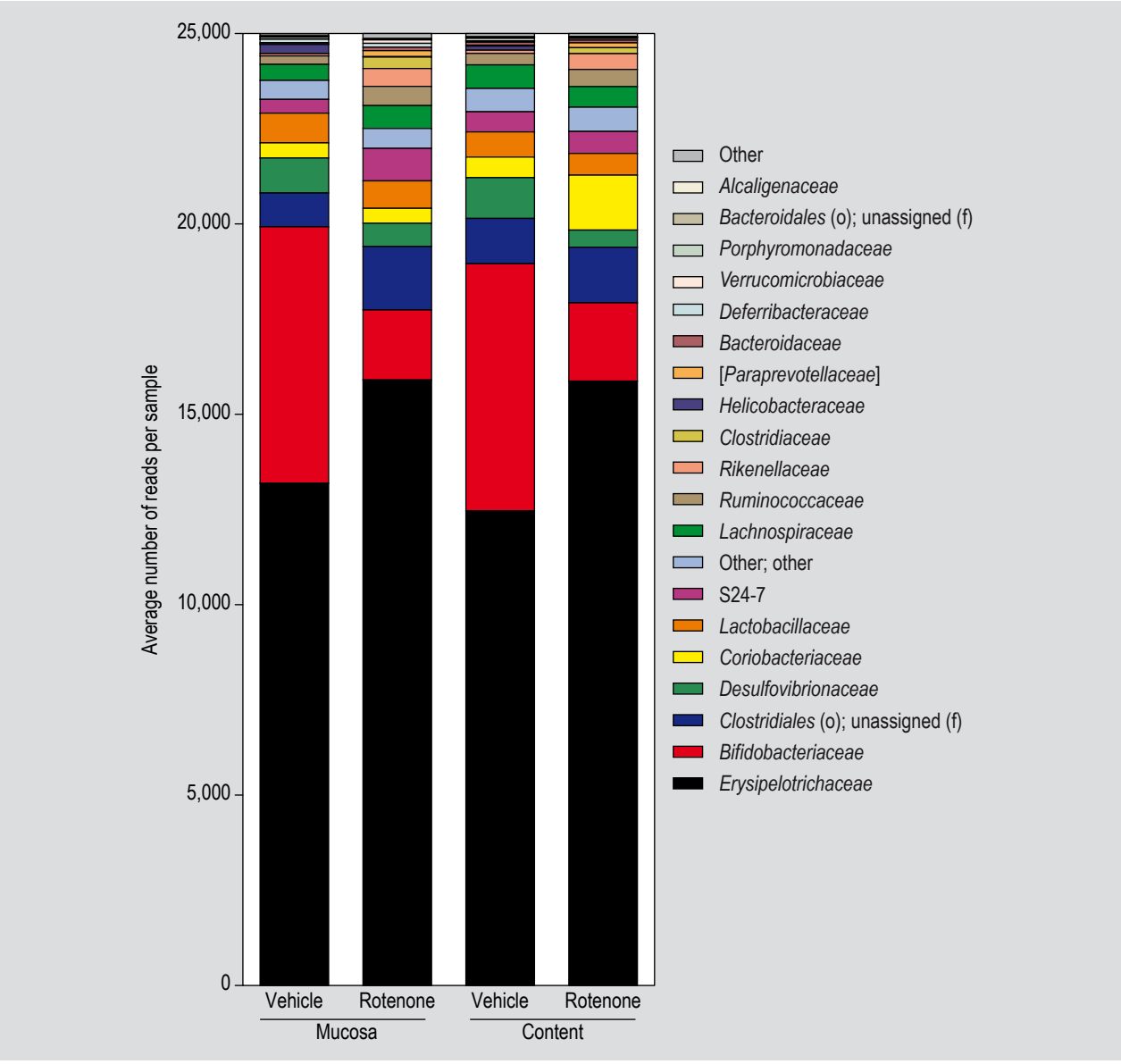

Figure 3. Stacked column plots depicting the average number of microbial reads per sample, at the taxonomic level of family.

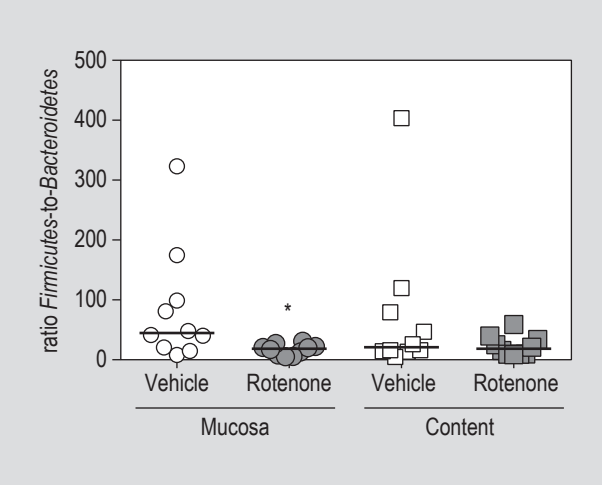

Figure 4. *Firmicutes*-to-*Bacteriodetes* ratio comparisons between vehicle and rotenone treated mice caecal mucosa and content, at the taxonomic level of phylum. Data are expressed as mean + standard error of the mean and analysed with 2-way ANOVA – Bonferroni post-hoc test for n=9-10 per group; * *P*=0.05 (site); ** *P*=0.01 (treatment).

Additionally, the caecal mucosa of the rotenone-treated mice showed a significant (FDR-P<0.05) increase in the relative abundances in associated annotated taxonomic families: *Rikenellaceae*, S24-7, *Clostridiales*_Unclassified, Ruminococcaceae and genus *Allobaculum* (Table 1, Figure 3, and Figure 5). Furthermore, rotenone-treated mice showed a significant decrease in the relative abundance of the genus *Bifidobacterium* in the caecal mucosa, compared to vehicle-treated mice (Figure 5). Additionally, these individual caecum mucosa taxa differences mentioned were similar to the changes seen in the caecal content taxa, between rotenone-treated and vehicle-treated mice. Together, these beta diversity results suggest that the rotenone treatment significantly affected both the caecal mucosa associated and luminal microbiota community structure (Figure 5 and Table 1). These changes in microbiota composition such as decreased F/B ratio, increased relative abundance of putative pro-inflammatory bacteria *Rikenellaceae* and *Allobaculum* and decreased relative abundance of putative anti-inflammatory bacteria *Bifidobacterium,* are also compatible with a putative pro-inflammatory dysbiotic microbiota community in rotenone-treated mice.

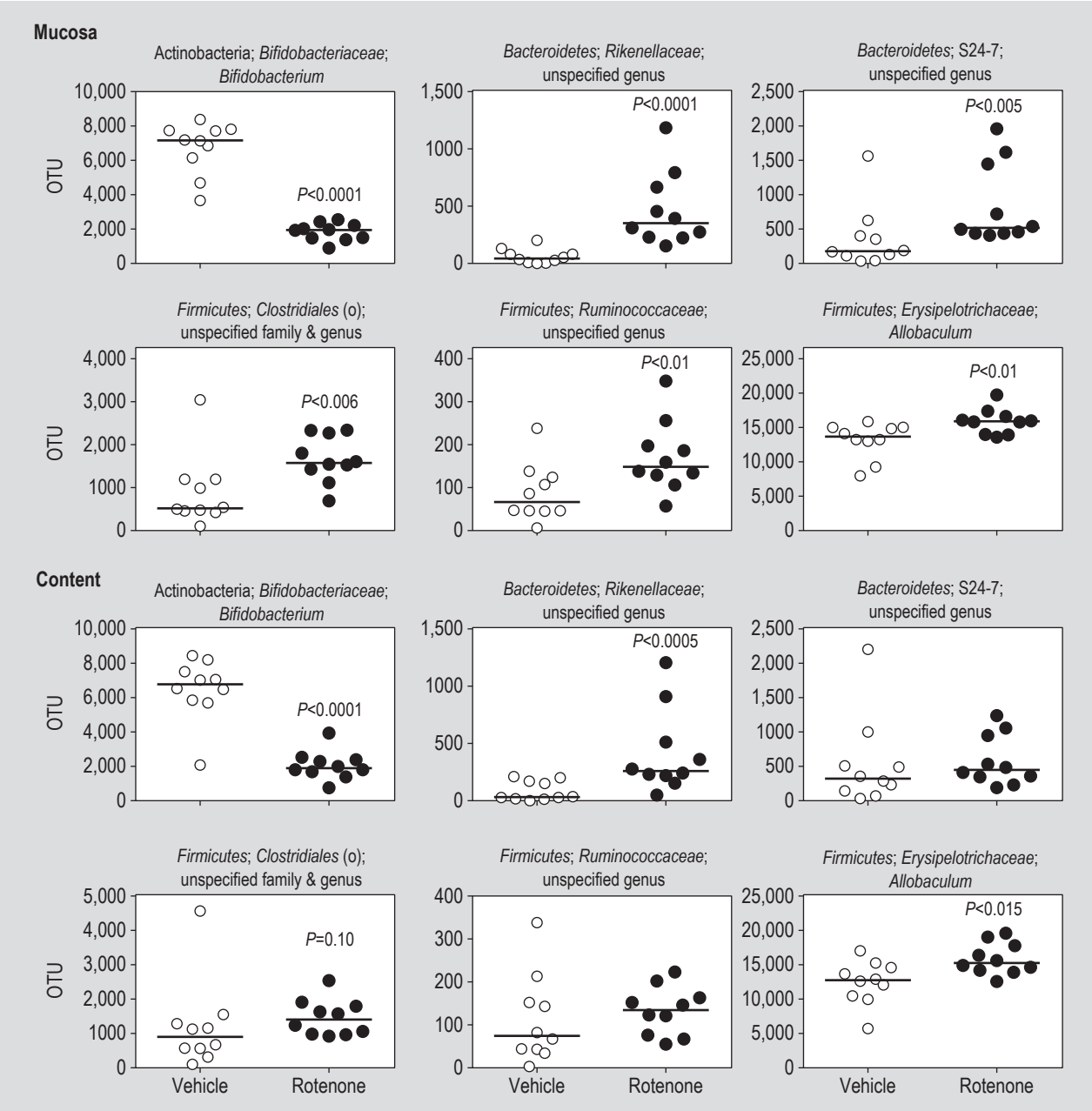

Figure 5. Effect of rotenone on operational taxonomic units (OTUs) of caecal mucosa-associated and content bacteria in mice. Mice were orally treated with rotenone (black dots) or vehicle (white dots). Data are expressed as median and analysed with non-parametric Mann Whitney U test for n=9-10 per group.

Evidence to support the microbiota-gut-brain axis involvement in rotenone-induced PD mice

In an effort to understand how multiple variables are similar or dissimilar from each other, correlation analysis was performed at the taxonomic level of family. While a correlation does not equate to causation, these relationships allow us to infer potential relationships. First, correlations were assessed to investigate the association between caecal bacterial content and intestinal barrier integrity, inflammation and alpha-synuclein accumulation in the ENS. The intestinal epithelial barrier integrity score, assessed by ZO-1 expression, significantly positively correlated with the taxonomic level family *Bifidobacteriaceae*, and negatively correlated with taxonomic level families: *Rikenellaceae*, S24-7, unassigned family of the order *Clostridiales*, and *Ruminococcaceae* in the caecal mucosa (Table 2, Supplementary Figure S1). Caecal content correlations were similar, except for S24-7 and unassigned family of the order *Clostridiales*, where no significant correlations with ZO-1 expression. The number of CD3+ T-cells in the colon, (i.e. a marker of intestinal inflammation/immune activation) and epithelial barrier integrity score both, correlated with these similar bacterial taxonomic families in both caecal sample sites. In addition, *Ruminococcaceae*, in the caecal content, did not correlate with CD3+ T-cells. The alpha-synuclein accumulation in the colonic plexi correlated with the above mentioned bacterial families in both the caecal mucosa and content as found for the intestinal epithelial barrier integrity score, with the exception of *Ruminococcaceae* in the caecal content (Table 2, Supplementary Figures S1 and S2).

Next, the correlation analysis was performed to investigate the association between caecal bacteria to neuroinflammation and dopaminergic cells loss in the SN. Microglial activation in the SN did not correlate with any bacterial family from caecal mucosa and content (Table 2). On the other hand, the dopaminergic cell number in the SN, assessed by the number of TH+ cells, was significantly inversely correlated with *Rikenellaceae*, *Erysipelotrichaceae*, *Ruminococcaceae* and S24-7 (only for mucosal associated bacteria), and positively correlated with *Bifidobacteriaceae* (Table 2, Supplementary Figure S1 and S2).

Functional prediction of microbiota associated metabolic pathways

Predictive assessment of the microbial community functional potential (PICRUSt) was used to infer functional differences in the microbiota of rotenone treated versus control mice. PICRUSt is a computational tool that allows, using 16S rRNA amplicon data, to predict the genes that are present, to calculate their abundance, assign them to metabolic pathways using KEGG and then test the difference between rotenone and vehicle treated mice. In caecal mucosa associated bacteria most KEGG pathways suggested more genes in the rotenone treated mice. Among all the tested metabolic pathways, twelve were suggested to be significantly upregulated and nine showed a suggestive trend when comparing rotenone-treated mice with controls. In particular, rotenone induced a significant (FDR-P<0.05) enhancement of the following pathways: glycan biosynthesis and metabolism; metabolism of terpenoids and polyketides; xenobiotics biodegradation and metabolism; metabolism of other amino acids; biosynthesis of other secondary metabolites amino acid metabolism lipid metabolism (Table 3). Only three metabolic pathways were found to be significantly downregulated (FDR-P<0.05) in the caecal mucosal-associated bacteria after rotenone treatment in mice: xenobiotics biodegradation and metabolism and metabolism of cofactors and vitamins (Table 3). For the caecal content associated bacteria, KEGG pathways had suggested fewer genes in the rotenone treated mice. Eight metabolic pathways were significantly downregulated (FDR-P<0.05) and four pathways showed a trend when comparing rotenone-treated mice with controls (Table 4). In particular, rotenone induced a significant (FDR-P<0.05) reduction of the following pathways: xenobiotics biodegradation and metabolism; metabolism of cofactors and vitamins; carbohydrate metabolism; amino acid metabolism and fatty acid metabolism (Table 4). No significantly different KEGG pathways with greater abundance in rotenone relative to vehicle treated mice were found.

4. Discussion

The intestinal microbiota composition (and its metabolites including short chain fatty acids (SCFAs)) is a major component of the gut-brain axis. If disrupted, the microbiota composition and function could lead to abnormal gut-brain axis interactions causing altered maturation and inflammatory capabilities of microglia and neurodegeneration (Erny *et al.*, 2015). Indeed, multiple studies have demonstrated dysbiosis in several neuro-behavioural disorders in patients and animal models, like depression/anxiety (Clapp *et al.*, 2017; Rogers *et al.*, 2016), PTSD (Leclercq *et al.*, 2016), multiple sclerosis (Miyake *et al.*, 2015), multiple system atrophy (Engen *et al.*, 2017), autism spectrum disorders (Li *et al.*, 2017), impaired cognition (Fröhlich *et al.*, 2016) and of course PD (Keshavarzian *et al.*, 2015).

This is the first study investigating changes in both caecal mucosa and caecal content microbiota compositions, and possibly associated metabolic pathways in a mouse model for PD. We found that rotenone treated mice have putative pro-inflammatory dysbiotic mucosa associated and luminal microbiota communities, and the dysbiotic microbiota correlated with PD like functional and pathological changes in both the intestine and the brain.

Table 2. Correlations between intestinal barrier dysfunction (ZO-1 scoring data); colonic T-cell infiltration (CD3+ cells in colon); accumulation of alpha-synuclein in enteric plexi of colon; microglial activation and dopaminergic cells loss (loss of TH+cells) in substantia nigra (SN) with those bacterial family associated with caecal mucosa or found in the caecal content that were changed by rotenone treatment expressed as Pearson correlation coefficients.[1]

Phylum	Class	Order	Family	Mucosa				
				ZO-1 expression in colon	CD3+ cells in colon	α-synuclein in colonic plexi	microglial activation SN	number TH+ cells SN
Actinobacteria	*Actinobacteria*	*Bifidobacteriales*	*Bifidobacteriaceae*	r=0.79	r=-0.77	r=-0.77	r=-0.22	r=0.80
				P<0.0001	*P*<0.0001	*P*<0.0001	ns	*P*<0.0001
Bacteriodetes	*Bacteroidia*	*Bacteroidales*	*Rikenellaceae*	r=-0.67	r=0.77	r=0.68	r=0.54	r=-0.68
				P=0.0011	*P*<0.0001	*P*=0.0010	*P*=0.0885	*P*=0.001
			S24-7	r=-0.47	r=0.63	r=0.38	r=0.08	r=-0.38
				P=0.0346	*P*=0.0032	*P*=0.0962	ns	*P*=0.0960
Firmicutes	*Clostridia*	*Clorstridiales*	-	r=-0.51	r=0.40	r=0.54	r=-0.06	r=-0.30
				P=0.0217	*P*=0.0782	*P*=0.0134	ns	ns
			Lachnospiraceae	r=-0.25	r=0.19	r=0.17	r=-0.13	r=0.01
				ns	ns	ns	ns	ns
			Ruminoccaceae	r=-0.72	r=0.67	r=0.64	r=-0.01	r=-0.41
				P=0.0003	*P*=0.0012	*P*=0.021	ns	*P*=0.0691
	Erysipelotrichi	*Erysipelotrichales*	*Erysipelotrichaceae*	r=-0.40	r=0.35	r=0.42	r=0.22	r=-0.63
				P=0.0822	ns	*P*=0.0614	ns	*P*=0.0030
				Content				
				ZO-1 expression in colon	CD3+ cells in colon	α-synuclein in colonic plexi	microglial activation SN	number TH+ cells SN
Actinobacteria	*Actinobacteria*	*Bifidobacteriales*	*Bifidobacteriaceae*	r=0.72	r=-0.74	r=-0.73	r=-0.22	r=0.78
				P=0.0003	*P*=0.0002	*P*=0.0003	ns	*P*<0.0001
Bacteriodetes	*Bacteroidia*	*Bacteroidales*	*Rikenellaceae*	r=-0.54	r=0.56	r=0.52	r=0.57	r=-0.62
				P=0.0142	*P*=0.0097	*P*=0.0176	*P*=0.0689	*P*=0.0038
			S24-7	r=-0.10	r=0.20	r=-0.01	r=-0.09	r=-0.06
				ns	ns	ns	ns	ns
Firmicutes	*Clostridia*	*Clorstridiales*	-	r=-0.15	r=0.14	r=0.23	r=-0.17	r=-0.19
				ns	ns	ns	ns	ns
			Lachnospiraceae	r=0.08	r=-0.02	r=-0.04	r=-0.43	r=-0.00
				ns	ns	ns	ns	ns
			Ruminoccaceae	r=-0.46	r=0.32	r=0.35	r=-0.11	r=-0.17
				P=0.0430	ns	ns	ns	ns
	Erysipelotrichi	*Erysipelotrichales*	*Erysipelotrichaceae*	r=-0.46	r=0.36	r=0.52	r=0.47	r=-0.46
				P=0.0395	ns	*P*=0.0180	ns	*P*=0.0437

[1] Significant difference *P*<0.05: trend *P*≤0.10. See Supplementary Figure S1 and S2 for scatter plots of all significant correlations.

Table 3. List of different KEGG pathways with greater abundance in rotenone relative to vehicle treated wildtype (WT) mice & greater abundance in vehicle relative to rotenone treated WT mice, as inferred using PICRUSt analysis of caecal mucosal microbiomes.

Pathway caecum mucosa[1]		FDR-*P*-value[2]	Abundance mean, rotenone WT	Abundance mean, vehicle WT	rotenone/vehicle ratio
gbm	glycosphingolipid biosynthesis – ganglio series	0.05	4,956	1,516	3.27
gbm	glycosaminoglycan degradation	0.04	7,945	2,477	3.21
mtp	biosynthesis of siderophore group nonribosomal peptides	0.04	1,180	483	2.44
xbm	atrazine degradation	0.07	2,976	1,592	1.87
xbm	caprolactam degradation	0.10	3,436	2,054	1.67
xbm	styrene degradation	0.09	2,322	1,413	1.64
moa	beta-alanine metabolism	0.05	29,818	19,531	1.53
	sporulation	0.09	81,254	54,120	1.50
xbm	aminobenzoate degradation	0.05	25,969	17,778	1.46
bsm	butirosin and neomycin biosynthesis	0.05	13,650	9,429	1.45
aam	lysine degradation	0.05	38,598	26,753	1.44
lm	lipid metabolism	0.05	18,865	13,190	1.43
bsm	biosynthesis and biodegradation of secondary metabolites	0.05	13,581	9,641	1.41
aam	amino acid metabolism	0.05	51,344	37,920	1.35
aam	tryptophan metabolism	0.08	42,834	32,187	1.33
mt	phosphotransferase system	0.08	336,956	254,162	1.33
xbm	bisphenol degradation	0.05	22,504	17,193	1.31
mcv	porphyrin and chlorophyll metabolism	0.08	120,779	92,810	1.30
moa	cyanoamino acid metabolism	0.08	50,406	38,980	1.29
lm	glycerolipid metabolism	0.05	98,758	78,235	1.26
xbm	nitrotoluene degradation	0.07	15,314	12,352	1.24
			Abundance mean, vehicle WT	**Abundance mean, rotenone WT**	**vehicle/rotenone ratio**
xbm	chlorocyclohexane and chlorobenzene degradation	0.01	6,763	2,847	2.38
mcv	retinol metabolism	0.01	8,011	3,648	2.20
xbm	metabolism of xenobiotics by cytochrome P450	0.02	7,823	3,664	2.13

[1] aam = amino acid metabolism; bsm = biosynthesis of other secondary metabolites; cm = carbohydrate metabolism; fam = fatty acid metabolism; gbm = glycanbiosynthesis and metabolism; lm = lipid metabolism; mcv = metabolism of cofactors and vitamins; moa = metabolism of other amino acids; mt = membrane transport; mtp = metabolism of terpenoids and polyketides; xbm = xenobiotics biodegradation and metabolism.
[2] $P<0.05$, significant different; $P\leq0.10$, trend.

Our group has previously shown that oral exposure to rotenone induced intestinal dysfunction and inflammation in the colon (Perez-Pardo *et al.*, 2017). Others have shown that chronic administration of rotenone in rodents caused gut inflammation, a decrease in stool frequency and delayed gastric emptying (Greene *et al.*, 2009; Pan-Montojo *et al.*, 2010). Tasselli *et al.* (2013) also showed that the repeated oral administration of rotenone in mice decreased faecal pellet output, but they could not detect changes in gastric emptying or total intestinal transit. Yang *et al.* (2017) showed changes in faecal microbiome (dysbiosis characterised by an overall decrease in bacterial diversity and a significant change of microbiota composition) and pathologic processes, using a rotenone-induced PD mice model over a period of four weeks. Moreover, rotenone-induced GI and motor dysfunctions correlated with changes in the composition of faecal microbiota. Very recently, Johnson *et al.* (2018) demonstrated that intraperitoneal rotenone administration in rats alters small intestinal and colonic microbiome composition and reproduces clinical symptoms of gastroparesis before nigrostriatal pathology is evident.

Here, we show rotenone treatment associated microbiome changes at different taxonomic levels in the cecum's mucosa and luminal content of a PD mice model. The murine microbiota compositions of caecal mucosa-associated and caecal content were more or less similar regardless

Table 4. List of different KEGG pathways with greater abundance in vehicle relative to rotenone treated WT mice, as inferred using PICRUSt analysis of caecum content microbiomes.[1]

Pathway caecum content[2]		FDR-*P*-value[3]	Abundance mean, vehicle WT	Abundance mean, rotenone WT	vehicle/rotenone ratio
xbm	chlorocyclohexane and chlorobenzene degradation	0.01	8,078	3,191	2.53
mcv	retinol metabolism	0.01	9,561	3,781	2.53
xbm	metabolism of xenobiotics by cytochrome P450	0.01	9,450	3,768	2.51
xbm	xylene degradation	0.02	15,011	7,748	1.94
xbm	dioxin degradation	0.02	15,092	7,883	1.91
xbm	naphthalene degradation	0.02	30,669	17,127	1.79
mcv	lipoic acid metabolism	0.04	6,852	4,283	1.60
xbm	toluene degradation	0.10	16,909	10,616	1.59
cm	C5-branched dibasic acid metabolism	0.10	57,449	36,995	1.55
aam	valine, leucine and isoleucine biosynthesis	0.08	152,653	112,703	1.35
xbm	chloroalkane and chloroalkene degradation	0.04	60,944	45,352	1.34
fam	fatty acid metabolism	0.06	73,741	57,431	1.28

[1] No significantly different KEGG pathways with greater abundance in rotenone relative to vehicle treated mice were found.
[2] aam = amino acid metabolism; cm = carbohydrate metabolism; fam = fatty acid metabolism; mcv = metabolism of cofactors and vitamins; xbm = xenobiotics biodegradation and metabolism.
[3] $P<0.05$, significant different; $P\leq0.10$, trend.

of the treatment. All in all, the effects of rotenone were more pronounced on the mucosa-associated microbiota composition. This could be explained by the direct epithelium damaging effects of rotenone leading to a disruption of the microbiota-host interaction.

Rotenone-induced dysbiosis can (further) disrupt the epithelial integrity, leading to gut leakiness, innate immune activation and possibly systemic inflammation (Caricilli *et al.*, 2014; Ivanov and Honda, 2012; Nishio and Honda, 2012). Enhanced exposure to more putative pro-inflammatory bacteria and their products, originated from the caecum and possibly the colon, might activate mucosal immune cells that in turn can modulate the local and remote (upper intestinal tract and even other organs) immune responses (Lathrop *et al.*, 2011). Pro-inflammatory bacteria and/or bacterial products, such as lipopolysaccharides, might induce inflammation, immune activation and the associated oxidative stress locally in the intestinal tract, but possibly also remotely in the brain (Cryan and Dinan, 2012). Oxidative stress could initiate alpha-synuclein pathology in the ENS (Shults, 2006) that could spread in a prion-like fashion through connected neurons to the SN (Braak and Del Tredici, 2008; Desplats *et al.*, 2009; Hawkes *et al.*, 2009; Holmqvist *et al.*, 2014). Moreover, gut-derived bacterial products or the peripheral inflammatory response could impact the brain through systemic mechanisms. Indeed, the relative abundances of putative pro-inflammatory bacteria were increased in our rotenone-treated mice: family/(genus) *Rikenellaceae* (unspecified genus) and *Erysipelotrichaceae* (*Allobaculum*). Mice fed with a high fat diet developed an increased abundance of *Rikenellaceae* and colonic inflammation (Kim *et al.*, 2012). This high fat diet-induced increase of *Rikenellaceae* might exacerbate inflammation via the TLR4 signalling pathway. *Erysipelotrichaceae* (*Allobaculum*) has been shown to be positively correlated with intestinal inflammation and leaky gut, induced by high cholesterol diet in rats (Lee *et al.*, 2015). In addition, western type diet induced overweight, leaky gut and intestinal inflammation is also associated with high levels of *Allobaculum* (Boudry *et al.*, 2017). Taken together, the enhanced abundance of *Erysipelotrichaceae* in the rotenone-induced PD model might be involved in the intestinal inflammatory response.

At the family level, significant correlations between rotenone-associated microbial changes and intestinal inflammation and enteric alpha-synuclein pathology were found, supporting the importance of the microbiota in local immune responses. We acknowledge that alpha-synuclein pathology is not specific for PD and can be seen in the intestine and brain of other neurological disorders like Parkinsonism, including multiple system atrophy (Prusiner *et al.*, 2015; Yoshida, 2007) and lewy body dementia (Campbell *et al.*, 2000) and even in autopsy/biopsy samples from individuals with no history of PD (Gray *et al.*, 2014; Visanji *et al.*, 2015). Additionally, neuroinflammation and dopaminergic cells loss in the SN also correlated with several bacterial families. This suggests that the CNS response in the mouse model for PD might be regulated by

specific pro-inflammatory bacteria. Recent studies in mice overexpressing alpha-synuclein support the importance of the microbiota in PD symptoms development. Germ-free or antibiotic treated alpha-synuclein overexpressing mice were protected against neuroinflammation and motor dysfunction (Sampson *et al.*, 2016).

Yang and colleagues analysed faecal microbiome using an oral rotenone model of PD from a longitudinal study over a period of 4 weeks in male C57BL/6 mice, aged between 8 and 9 weeks. After 4 weeks of rotenone, they found a decrease in Simpson's diversity, with microbial shifts at the main bacterial phyla, resulting in an increased F/B ratio (*Firmicutes* increased; *Bacteroidetes* decreased) (Yang *et al.*, 2017). In comparison, our C57BL/6 mice, aged seven weeks, indicated increased richness (only caecal mucosa), pertaining to alpha diversity after 4 weeks of oral rotenone. The relative abundance of *Firmicutes* was also increased (both caecal sites) in our study. In contrast to Yang *et al.* (2017), the relative abundances of *Bacteroidetes* increased (both caecal sites), *Actinobacteria* decreased (both caecal sites), and the F/B ratio decreased (only caecal mucosa) in our rotenone-treated mice. Furthermore, Yang *et al.* (2017) faecal genus individual taxa differences were not significantly different in our caecum mucosal and content rodent model. The variability between studies could be attributed to three major factors: (1) different rotenone oral dose concentrations; Yang *et al.* (2017) administered a high rotenone dose of 30 mg/kg, while we gavaged a low rotenone dose of 10 mg/kg. (2) different GI sites; Yang *et al.* (2017) studied faeces, while we studied both caecum mucosal and luminal (caecum content). Previous microbiota studies have shown that sample collection from different areas of the GIT, produce significantly different overall microbial compositions (Carroll *et al.*, 2011; Durbán *et al.*, 2011; Engen *et al.*, 2017; Keshavarzian *et al.*, 2015). (3) different sequencing techniques; Yang *et al.* (2017) study sequences the V4 and V5 regions, while we sequenced only the V4 region.

It should be noted that direct comparison of microbiota data in rodents with human is not appropriate because major differences in the environments of human and rodents, such as diet, and the fact that environmental factors have a major impact on microbiota community (Nguyen *et al.*, 2015). Indeed, even comparisons of microbiota read outs in mice between different laboratories can lead to inaccurate conclusions due to different methods of sample collection (Hufeldt *et al.*, 2010), site of samples (caecal content, stool or mucosa), method of microbiota interrogation and environment (so called cage effects) (Hildebrand *et al.*, 2013; Laukens *et al.*, 2016). None the less, when we compared our study to human PD microbiota studies, we found few similarities, however; overall both rodent PD models and PD patients both had a putative 'pro-inflammatory' dysbiotic microbial community. Of note, at the taxonomic level of genus, our rotenone-treated mice exhibited a significant lower abundance of *Bifidobacterium* at both caecal sites. Recently, Minato *et al.* (2017) analysed 36 PD patients faecal microbiota and suggested that *Bifidobacterium* might play a protective role against psychic symptoms, which would be explained by its antioxidant effect and its contribution to the release of serotonin in the brain. A deficit of *Bifidobacterium* in subjects with Parkinson's disease might be a predictive factor for symptom worsening in a two-year period (Minato *et al.*, 2017). Also consistent with our rotenone-treated mice caecal mucosa results, a trend toward a lower F/B ratio in PD patients was observed between PD and control groups faecal microbiota in the study by Keshavarzian *et al.* (2015).

There are several limitations in our study. First, we used PICRUSt analysis to infer changes in microbiota function and our findings should be confirmed by more robust techniques like shotgun metagenomics and metabolomics in the future studies. Second, future longitudinal and interventional studies are required to confirm our observed correlation between dysbiotic microbiota and PD, like functional and pathological changes in order to establish causal link between dysbiosis and PD pathology including microglia activation, alpha-synuclein misfolding/aggregates and DA loss. Third, we interrogated microbiota in the caecum and further studies are needed to determine whether microbiota communities in other GI sites, like small bowel, are affected by rotenone treatment and whether the changes in microbiota community in the stomach and small intestine correlate more robustly with the observed reduced transit time and disturbed stomach emptying (Perez-Pardo *et al.*, 2017). This has relevance to PD, because a subset of patients with PD have small intestinal bacterial overgrowth (Gabrielli *et al.*, 2011; Tan *et al.*, 2014).

In conclusion, the mouse model for PD induced by the pesticide rotenone is associated with dysbiotic mucosal and luminal microbiota community structures characterised by enhanced abundance of (human relevant) putative pro-inflammatory intestinal bacteria at the expense of beneficial commensal bacteria in caecal mucosa and caecal content. Also, the dysbiotic microbiota correlated with several aspects of PD like pathology and functional deficit in the intestine and brain.

Supplementary material

Supplementary material can be found online at https://doi.org/10.3920/BM2017.0202.

Figure S1. Graphical representation of the significant correlations between different parameters and bacterial families found in the caecal mucosa.

Figure S2. Graphical representation of the significant correlations between different parameters and bacterial families found in the caecal content.

References

Abbott, R.D., Petrovitch, H., White, L.R., Masaki, K.H., Tanner, C.M., Curb, J.D., Grandinetti, A., Blanchette, P.L., Popper, J.S. and Ross, G.W., 2001. Frequency of bowel movements and the future risk of Parkinson's disease. Neurology 57: 456-462.

Adams-Carr, K.L., Bestwick, J.P., Shribman, S., Lees, A., Schrag, A. and Noyce, A.J., 2016. Constipation preceding Parkinson's disease: a systematic review and meta-analysis. Journal of Neurology, Neurosurgery, and Psychiatry 87: 710-716.

Basson, A., Trotter, A., Rodriguez-Palacios, A. and Cominelli, F., 2016. Mucosal interactions between genetics, diet, and microbiome in inflammatory bowel disease. Frontiers in Immunology 7: 290.

Bedarf, J.R., Hildebrand, F., Coelho, L.P., Sunagawa, S., Bahram, M., Goeser, F., Bork, P. and Wüllner, U., 2017. Functional implications of microbial and viral gut metagenome changes in early stage L-DOPA-naïve Parkinson's disease patients. Genome Medicine 9: 39.

Boudry, G., Hamilton, M.K., Chichlowski, M., Wickramasinghe, S., Barile, D., Kalanetra, K.M., Mills, D.A. and Raybould, H.E., 2017. Bovine milk oligosaccharides decrease gut permeability and improve inflammation and microbial dysbiosis in diet-induced obese mice. Journal of Dairy Science 100: 2471-2481.

Braak, H. and Del Tredici, K., 2008. Nervous system pathology in sporadic Parkinson disease. Neurology 70: 1916-1925.

Brown, K., Abbott, D.W., Uwiera, R.R.E. and Inglis, G.D., 2017. Removal of the cecum affects intestinal fermentation, enteric bacterial community structure, and acute colitis in mice. Gut Microbes 11: 1-18.

Campbell, B.C., Li, Q.X., Culvenor, J.G., Jäkälä, P., Cappai, R., Beyreuther, K., Masters, C.L. and McLean, C.A., 2000. Accumulation of insoluble alpha-synuclein in dementia with Lewy bodies. Neurobiology of Disease 7: 192-200.

Canani, R.B., Costanzo, M.D., Leone, L., Pedata, M., Meli, R. and Calignano, A., 2011. Potential beneficial effects of butyrate in intestinal and extraintestinal diseases. World Journal of Gastroenterology 17: 1519-1528.

Caporaso, J.G., Kuczynski, J., Stombaugh, J., Bittinger, K., Bushman, F.D., Costello, E.K., Fierer, N., Peña, A.G., Goodrich, J.K., Gordon, J.I., Huttley, G.A., Kelley, S.T., Knights, D., Koenig, J.E., Ley, R.E., Lozupone, C.A., McDonald, D., Muegge, B.D., Pirrung, M., Reeder, J., Sevinsky, J.R., Turnbaugh, P.J., Walters, W.A., Widmann, J., Yatsunenko, T., Zaneveld, J. and Knight, R., 2010. QIIME allows analysis of high-throughput community sequencing data. Nature Methods 7: 335-336.

Caporaso, J.G., Lauber, C.L., Walters, W.A., Berg-Lyons, D., Huntley, J., Fierer, N., Owens, S.M., Betley, J., Fraser, L., Bauer, M., Gormley, N., Gilbert, J.A., Smith, G., Knight, R., 2012. Ultra-high-throughput microbial community analysis on the Illumina HiSeq and MiSeq platforms. ISME Journal 6: 1621-1624.

Caricilli, A.M., Castoldi, A. and Câmara, N.O.S., 2014. Intestinal barrier: a gentlemen's agreement between microbiota and immunity. World Journal of Gastrointestinal Pathophysiology 5: 18-32.

Carroll, I.M., Ringel-Kulka, T., Keku, T.O., Chang, Y.-H., Packey, C.D., Sartor, R.B. and Ringel, Y., 2011. Molecular analysis of the luminal- and mucosal-associated intestinal microbiota in diarrhea-predominant irritable bowel syndrome. American Journal of Physiology – Gastrointestinal and Liver Physiology 301: G799-807.

Chaudhuri, K.R. and Schapira, A.H.V., 2009. Non-motor symptoms of Parkinson's disease: dopaminergic pathophysiology and treatment. The Lancet Neurology 8: 464-474.

Clapp, M., Aurora, N., Herrera, L., Bhatia, M., Wilen, E. and Wakefield, S., 2017. Gut microbiota's effect on mental health: the gut-brain axis. Clinical Practice 7: 987.

Clarke, K.R., 1993. Non-parametric multivariate analyses of changes in community structure. Australian Journal of Ecology 18: 117-143.

Crossman, A.R., 1989. Neural mechanisms in disorders of movement. Comparative Biochemistry and Physiology A 93: 141-149.

Cryan, J.F. and Dinan, T.G., 2012. Mind-altering microorganisms: the impact of the gut microbiota on brain and behaviour. Nature Reviews Neuroscience 13: 701-712.

De Rijk, M.C., Launer, L.J., Berger, K., Breteler, M.M., Dartigues, J.F., Baldereschi, M., Fratiglioni, L., Lobo, A., Martinez-Lage, J., Trenkwalder, C. and Hofman, A., 2000. Prevalence of Parkinson's disease in Europe: a collaborative study of population-based cohorts. Neurologic Diseases in the Elderly Research Group. Neurology 54: S21-23.

Deleidi, M. and Gasser, T., 2013. The role of inflammation in sporadic and familial Parkinson's disease. Cellular and Molecular Life Sciences 70: 4259-4273.

Desplats, P., Lee, H.-J., Bae, E.-J., Patrick, C., Rockenstein, E., Crews, L., Spencer, B., Masliah, E. and Lee, S.-J., 2009. Inclusion formation and neuronal cell death through neuron-to-neuron transmission of alpha-synuclein. Proceedings of the National Academy of Sciences of the USA 106: 13010-13015.

Dias, V., Junn, E. and Mouradian, M.M., 2013. The role of oxidative stress in Parkinson's disease. Journal of Parkinson's Disease 3: 461-491.

Durbán, A., Abellán, J.J., Jiménez-Hernández, N., Ponce, M., Ponce, J., Sala, T., D'Auria, G., Latorre, A. and Moya, A., 2011. Assessing gut microbial diversity from feces and rectal mucosa. Microbial Ecology 61: 123-133.

Edgar, R.C., 2010. Search and clustering orders of magnitude faster than BLAST. Bioinformatics 26: 2460-2461.

Engen, P.A., Dodiya, H.B., Naqib, A., Forsyth, C.B., Green, S.J., Voigt, R.M., Kordower, J.H., Mutlu, E.A., Shannon, K.M. and Keshavarzian, A., 2017. The potential role of gut-derived inflammation in multiple system atrophy. Journal of Parkinson's Disease 7: 331-346.

Erny, D., Hrabě de Angelis, A.L., Jaitin, D., Wieghofer, P., Staszewski, O., David, E., Keren-Shaul, H., Mahlakoiv, T., Jakobshagen, K., Buch, T., Schwierzeck, V., Utermöhlen, O., Chun, E., Garrett, W.S., McCoy, K.D., Diefenbach, A., Staeheli, P., Stecher, B., Amit, I. and Prinz, M., 2015. Host microbiota constantly control maturation and function of microglia in the CNS. Nature Neuroscience 18: 965-977.

Fasano, A., Visanji, N.P., Liu, L.W.C., Lang, A.E. and Pfeiffer, R.F., 2015. Gastrointestinal dysfunction in Parkinson's disease. The Lancet Neurology 14: 625-639.

Forsyth, C.B., Shannon, K.M., Kordower, J.H., Voigt, R.M., Shaikh, M., Jaglin, J.A., Estes, J.D., Dodiya, H.B. and Keshavarzian, A., 2011. Increased intestinal permeability correlates with sigmoid mucosa alpha-synuclein staining and endotoxin exposure markers in early Parkinson's disease. PLoS ONE 6: e28032.

Fröhlich, E.E., Farzi, A., Mayerhofer, R., Reichmann, F., Jačan, A., Wagner, B., Zinser, E., Bordag, N., Magnes, C., Fröhlich, E., Kashofer, K., Gorkiewicz, G., Holzer, P., 2016. Cognitive impairment by antibiotic-induced gut dysbiosis: analysis of gut microbiota-brain communication. Brain, Behavior, and Immunity 56: 140-155.

Gabrielli, M., Bonazzi, P., Scarpellini, E., Bendia, E., Lauritano, E.C., Fasano, A., Ceravolo, M.G., Capecci, M., Rita Bentivoglio, A., Provinciali, L., Tonali, P.A. and Gasbarrini, A., 2011. Prevalence of small intestinal bacterial overgrowth in Parkinson's disease. Movement Disorders Journal 26: 889-892.

Gihring, T.M., Green, S.J. and Schadt, C.W., 2012. Massively parallel rRNA gene sequencing exacerbates the potential for biased community diversity comparisons due to variable library sizes. Environmental Microbiology 14: 285-290.

Glass, C.K., Saijo, K., Winner, B., Marchetto, M.C. and Gage, F.H., 2010. Mechanisms underlying inflammation in neurodegeneration. Cell 140: 918-934.

Gray, M.T., Munoz, D.G., Gray, D.A., Schlossmacher, M.G. and Woulfe, J.M., 2014. Alpha-synuclein in the appendiceal mucosa of neurologically intact subjects. Movement Disorders Journal 29: 991-998.

Greene, J.G., Noorian, A.R. and Srinivasan, S., 2009. Delayed gastric emptying and enteric nervous system dysfunction in the rotenone model of Parkinson's disease. Experimental Neurology 218: 154-161.

Guan, J., Pavlovic, D., Dalkie, N., Waldvogel, H.J., O'Carroll, S.J., Green, C.R. and Nicholson, L.F.B., 2013. Vascular degeneration in Parkinson's disease. Brain Pathology 23: 154-164.

Hakansson, A. and Molin, G., 2011. Gut microbiota and inflammation. Nutrients 3: 637-682.

Hasegawa, S., Goto, S., Tsuji, H., Okuno, T., Asahara, T., Nomoto, K., Shibata, A., Fujisawa, Y., Minato, T., Okamoto, A., Ohno, K. and Hirayama, M., 2015. Intestinal dysbiosis and lowered serum Lipopolysaccharide-binding protein in Parkinson's disease. PLoS ONE 10: e0142164.

Hawkes, C.H., Del Tredici, K. and Braak, H., 2010. A timeline for Parkinson's disease. Parkinsonism and Related Disorders 16: 79-84.

Hawkes, C.H., Del Tredici, K. and Braak, H., 2009. Parkinson's disease: the dual hit theory revisited. Annals of the N.Y. Academy of Sciences 1170: 615-622.

Hildebrand, F., Nguyen, T.L.A., Brinkman, B., Yunta, R.G., Cauwe, B., Vandenabeele, P., Liston, A. and Raes, J., 2013. Inflammation-associated enterotypes, host genotype, cage and inter-individual effects drive gut microbiota variation in common laboratory mice. Genome Biology 14: R4.

Hill-Burns, E.M., Debelius, J.W., Morton, J.T., Wissemann, W.T., Lewis, M.R., Wallen, Z.D., Peddada, S.D., Factor, S.A., Molho, E., Zabetian, C.P., Knight, R. and Payami, H., 2017. Parkinson's disease and Parkinson's disease medications have distinct signatures of the gut microbiome. Movement Disorders Journal 32: 739-749.

Hilton, D., Stephens, M., Kirk, L., Edwards, P., Potter, R., Zajicek, J., Broughton, E., Hagan, H. and Carroll, C., 2014. Accumulation of α-synuclein in the bowel of patients in the pre-clinical phase of Parkinson's disease. Acta Neuropathology 127: 235-241.

Holmqvist, S., Chutna, O., Bousset, L., Aldrin-Kirk, P., Li, W., Björklund, T., Wang, Z.-Y., Roybon, L., Melki, R., Li, J.-Y., 2014. Direct evidence of Parkinson pathology spread from the gastrointestinal tract to the brain in rats. Acta Neuropathology 128: 805-820.

Hopfner, F., Künstner, A., Müller, S.H., Künzel, S., Zeuner, K.E., Margraf, N.G., Deuschl, G., Baines, J.F. and Kuhlenbäumer, G., 2017. Gut microbiota in Parkinson disease in a northern German cohort. Brain Research 1667: 41-45.

Huang, X.-Z., Zhu, L.-B., Li, Z.-R. and Lin, J., 2013. Bacterial colonization and intestinal mucosal barrier development. World Journal of Clinical Pediatrics 2: 46-53.

Hufeldt, M.R., Nielsen, D.S., Vogensen, F.K., Midtvedt, T. and Hansen, A.K., 2010. Variation in the gut microbiota of laboratory mice is related to both genetic and environmental factors. Comparative Medicine 60: 336-347.

Ivanov, I.I. and Honda, K., 2012. Intestinal commensal microbes as immune modulators. Cell Host Microbe 12: 496-508.

Johnson, M.E., Stringer, A. and Bobrovskaya, L., 2018. Rotenone induces gastrointestinal pathology and microbiota alterations in a rat model of Parkinson's disease. Neurotoxicology 65: 174-185.

Kanehisa, M. and Goto, S., 2000. KEGG: kyoto encyclopedia of genes and genomes. Nucleic Acids Research 28: 27-30.

Kanehisa, M., Goto, S., Sato, Y., Furumichi, M. and Tanabe, M., 2012. KEGG for integration and interpretation of large-scale molecular data sets. Nucleic Acids Research 40: D109-114.

Kelly, L.P., Carvey, P.M., Keshavarzian, A., Shannon, K.M., Shaikh, M., Bakay, R.A.E. and Kordower, J.H., 2014. Progression of intestinal permeability changes and alpha-synuclein expression in a mouse model of Parkinson's disease. Movement Disorders Journal 29: 999-1009.

Keshavarzian, A., Green, S.J., Engen, P.A., Voigt, R.M., Naqib, A., Forsyth, C.B., Mutlu, E. and Shannon, K.M., 2015. Colonic bacterial composition in Parkinson's disease. Movement Disorders Journal 30: 1351-1360.

Kim, K.-A., Gu, W., Lee, I.-A., Joh, E.-H. and Kim, D.-H., 2012. High fat diet-induced gut microbiota exacerbates inflammation and obesity in mice via the TLR4 signaling pathway. PLoS ONE 7: e47713.

Kostic, A.D., Howitt, M.R. and Garrett, W.S., 2013. Exploring host-microbiota interactions in animal models and humans. Genes & Development 27: 701-718.

Langille, M.G.I., Zaneveld, J., Caporaso, J.G., McDonald, D., Knights, D., Reyes, J.A., Clemente, J.C., Burkepile, D.E., Vega Thurber, R.L., Knight, R., Beiko, R.G. and Huttenhower, C., 2013. Predictive functional profiling of microbial communities using 16S rRNA marker gene sequences. Nature Biotechnology 31: 814-821.

Lathrop, S.K., Bloom, S.M., Rao, S.M., Nutsch, K., Lio, C.-W., Santacruz, N., Peterson, D.A., Stappenbeck, T.S. and Hsieh, C.-S., 2011. Peripheral education of the immune system by colonic commensal microbiota. Nature 478: 250-254.

Laukens, D., Brinkman, B.M., Raes, J., De Vos, M. and Vandenabeele, P., 2016. Heterogeneity of the gut microbiome in mice: guidelines for optimizing experimental design. FEMS Microbiology Reviews 40: 117-132.

Leclercq, S., Forsythe, P. and Bienenstock, J., 2016. Posttraumatic Stress Disorder: does the gut microbiome hold the key? Canadian Journal of Psychiatry 61: 204-213.

Lee, S.-M., Han, H.W. and Yim, S.Y., 2015. Beneficial effects of soy milk and fiber on high cholesterol diet-induced alteration of gut microbiota and inflammatory gene expression in rats. Food & Function 6: 492-500.

Li, Q., Han, Y., Dy, A.B.C. and Hagerman, R.J., 2017. The gut microbiota and autism spectrum disorders. Frontiers in Cellular Neuroscience 11: 120.

Li, W., Wu, X., Hu, X., Wang, T., Liang, S., Duan, Y., Jin, F. and Qin, B., 2017. Structural changes of gut microbiota in Parkinson's disease and its correlation with clinical features. Science China Life Sciences 60: 1223-1233.

Louis, P. and Flint, H.J., 2009. Diversity, metabolism and microbial ecology of butyrate-producing bacteria from the human large intestine. FEMS Microbiology Letters 294: 1-8.

Luna, E. and Luk, K.C., 2015. Bent out of shape: α-Synuclein misfolding and the convergence of pathogenic pathways in Parkinson's disease. FEBS Letters 589: 3749-3759.

Macfarlane, S. and Macfarlane, G.T., 2003. Regulation of short-chain fatty acid production. Proceedings of the Nutrition Society 62: 67-72.

Martinez-Martin, P., 2011. The importance of non-motor disturbances to quality of life in Parkinson's disease. Journal of the Neurological Sciences 310: 12-16.

McDermott, A.J. and Huffnagle, G.B., 2014. The microbiome and regulation of mucosal immunity. Immunology 142: 24-31.

McDonald, D., Clemente, J.C., Kuczynski, J., Rideout, J.R., Stombaugh, J., Wendel, D., Wilke, A., Huse, S., Hufnagle, J., Meyer, F., Knight, R. and Caporaso, J.G., 2012. The Biological Observation Matrix (BIOM) format or: how I learned to stop worrying and love the ome-ome. GigaScience 1: 7.

Minato, T., Maeda, T., Fujisawa, Y., Tsuji, H., Nomoto, K., Ohno, K. and Hirayama, M., 2017. Progression of Parkinson's disease is associated with gut dysbiosis: two-year follow-up study. PLoS ONE 12: e0187307.

Miyake, S., Kim, S., Suda, W., Oshima, K., Nakamura, M., Matsuoka, T., Chihara, N., Tomita, A., Sato, W., Kim, S.-W., Morita, H., Hattori, M. and Yamamura, T., 2015. Dysbiosis in the gut microbiota of patients with multiple sclerosis, with a striking depletion of species belonging to clostridia XIVa and IV clusters. PLoS ONE 10: e0137429.

Müller, B., Assmus, J., Herlofson, K., Larsen, J.P. and Tysnes, O.-B., 2013. Importance of motor vs. non-motor symptoms for health-related quality of life in early Parkinson's disease. Parkinsonism and Related Disorders 19: 1027-1032.

Nguyen, T.L.A., Vieira-Silva, S., Liston, A. and Raes, J., 2015. How informative is the mouse for human gut microbiota research? Disease Models & Mechanisms 8: 1-16.

Nishio, J. and Honda, K., 2012. Immunoregulation by the gut microbiota. Cellular and Molecular Life Sciences 69: 3635-3650.

Nussbaum, R.L. and Ellis, C.E., 2003. Alzheimer's disease and Parkinson's disease. New England Journal of Medicine 348: 1356-1364.

Pan-Montojo, F., Anichtchik, O., Dening, Y., Knels, L., Pursche, S., Jung, R., Jackson, S., Gille, G., Spillantini, M.G., Reichmann, H., Funk, R.H.W., 2010. Progression of Parkinson's disease pathology is reproduced by intragastric administration of rotenone in mice. PLoS ONE 5: e8762.

Perez-Pardo, P., Dodiya, H.B., Broersen, L.M., Douna, H., Van Wijk, N., Lopes da Silva, S., Garssen, J., Keshavarzian, A. and Kraneveld, A.D., 2017. Gut-brain and brain-gut axis in Parkinson's disease models: effects of a uridine and fish oil diet. Nutritional Neuroscience 9: 1-12.

Petrov, V.A., Saltykova, I.V., Zhukova, I.A., Alifirova, V.M., Zhukova, N.G., Dorofeeva, Y.B., Tyakht, A.V., Kovarsky, B.A., Alekseev, D.G., Kostryukova, E.S., Mironova, Y.S., Izhboldina, O.P., Nikitina, M.A., Perevozchikova, T.V., Fait, E.A., Babenko, V.V., Vakhitova, M.T., Govorun, V.M. and Sazonov, A.E., 2017. Analysis of gut microbiota in patients with Parkinson's disease. Bulletin of Experimental Biology and Medicine 162: 734-737.

Pfeiffer, R.F., 2011. Gastrointestinal dysfunction in Parkinson's disease. Parkinsonism and Related Disorders 17: 10-15.

Prusiner, S.B., Woerman, A.L., Mordes, D.A., Watts, J.C., Rampersaud, R., Berry, D.B., Patel, S., Oehler, A., Lowe, J.K., Kravitz, S.N., Geschwind, D.H., Glidden, D.V., Halliday, G.M., Middleton, L.T., Gentleman, S.M., Grinberg, L.T. and Giles, K., 2015. Evidence for α-synuclein prions causing multiple system atrophy in humans with parkinsonism. Proceedings of the National Academy of Sciences of the USA 112: E5308-5317.

Ransohoff, R.M., 2016. How neuroinflammation contributes to neurodegeneration. Science 353: 777-783.

Rogers, G.B., Keating, D.J., Young, R.L., Wong, M.-L., Licinio, J. and Wesselingh, S., 2016. From gut dysbiosis to altered brain function and mental illness: mechanisms and pathways. Molecular Psychiatry 21: 738-748.

Sampson, T.R., Debelius, J.W., Thron, T., Janssen, S., Shastri, G.G., Ilhan, Z.E., Challis, C., Schretter, C.E., Rocha, S., Gradinaru, V., Chesselet, M.-F., Keshavarzian, A., Shannon, K.M., Krajmalnik-Brown, R., Wittung-Stafshede, P., Knight, R. and Mazmanian, S.K., 2016. Gut microbiota regulate motor deficits and neuroinflammation in a model of Parkinson's disease. Cell 167: 1469-1480.

Scheperjans, F., Aho, V., Pereira, P.A.B., Koskinen, K., Paulin, L., Pekkonen, E., Haapaniemi, E., Kaakkola, S., Eerola-Rautio, J., Pohja, M., Kinnunen, E., Murros, K. and Auvinen, P., 2015. Gut microbiota are related to Parkinson's disease and clinical phenotype. Movement Disorders Journal 30: 350-358.

Shannon, K.M., Keshavarzian, A., Dodiya, H.B., Jakate, S. and Kordower, J.H., 2012. Is alpha-synuclein in the colon a biomarker for premotor Parkinson's disease? Evidence from 3 cases. Movement Disorders Journal 27: 716-719.

Shults, C.W., 2006. Lewy bodies. Proceedings of the National Academy of Sciences of the USA 103: 1661-1668.

Stokholm, M.G., Danielsen, E.H., Hamilton-Dutoit, S.J. and Borghammer, P., 2016. Pathological α-synuclein in gastrointestinal tissues from prodromal Parkinson disease patients. Annals of Neurology 79: 940-949.

Tan, A.H., Mahadeva, S., Thalha, A.M., Gibson, P.R., Kiew, C.K., Yeat, C.M., Ng, S.W., Ang, S.P., Chow, S.K., Tan, C.T., Yong, H.S., Marras, C., Fox, S.H., Lim, S.-Y., 2014. Small intestinal bacterial overgrowth in Parkinson's disease. Parkinsonism and Related Disorders 20: 535-540.

Tasselli, M., Chaumette, T., Paillusson, S., Monnet, Y., Lafoux, A., Huchet-Cadiou, C., Aubert, P., Hunot, S., Derkinderen, P. and Neunlist, M., 2013. Effects of oral administration of rotenone on gastrointestinal functions in mice. Journal of Neurogastroenterology and Motility 25: e183-193.

Unger, M.M., Spiegel, J., Dillmann, K.-U., Grundmann, D., Philippeit, H., Bürmann, J., Faβbender, K., Schwiertz, A. and Schäfer, K.-H., 2016. Short chain fatty acids and gut microbiota differ between patients with Parkinson's disease and age-matched controls. Parkinsonism and Related Disorders 32: 66-72.

Visanji, N.P., Marras, C., Kern, D.S., Al Dakheel, A., Gao, A., Liu, L.W.C., Lang, A.E., Hazrati, L.-N., 2015. Colonic mucosal a-synuclein lacks specificity as a biomarker for Parkinson disease. Neurology 84: 609-616.

Wexler, H.M., 2007. Bacteroides: the good, the bad, and the nitty-gritty. Clinical Microbiology Reviews 20: 593-621.

Yang, X., Qian, Y., Xu, S., Song, Y. and Xiao, Q., 2017. Longitudinal analysis of fecal microbiome and pathologic processes in a rotenone induced mice model of Parkinson's disease. Frontiers in Aging Neuroscience 9: 441.

Yoshida, M., 2007. Multiple system atrophy: alpha-synuclein and neuronal degeneration. Neuropathology 27: 484-493.